



OREGON STATE UNIVERSITY

2019 NASA SL TEAM

104 KERR ADMIN BLDG. # 1011

CORVALLIS, OR 97331

FRR Report Addendum

March 25th, 2019

CONTENTS

1	Summary of FRR Addendum Report	6
1.1	Team Summary	6
1.2	Purpose of Flight	6
1.3	Flight Summary Information	6
1.3.1	Launch Day Conditions	6
1.3.2	Vehicle Configuration Summary	7
1.3.3	Payload & Mission Summary	7
1.3.4	Flight Altitude Summary	7
1.3.5	Off-Nominal Events	8
1.4	Changes Made Since FRR	8
2	Payload Demonstration Flight Results	9
2.1	Payload Retention and Ejection System	9
2.1.1	System Design	9
2.1.2	Retention and Ejection Performance	12
2.2	Payload Mission	17
2.2.1	Rover Mission Summary	17
2.2.2	Rover Performance	17
2.2.3	Rover Lessons Learned	18
3	Flight Summary	19
3.1	Functional Systems	19
3.2	Malfunctioning Systems	19
3.3	Mission Performance Predictions	21
3.3.1	Flight Profile Simulations	21
3.3.2	Stability Margin	21
3.3.3	Simulated Kinetic Energy	21
3.3.4	Simulated Descent Time	22
3.3.5	Simulated Drift	23
3.4	Flight Results	23
3.4.1	Flight Profile	23
3.4.2	Kinetic Energy and Descent Times	25
3.4.3	Drift	27
3.4.4	Drag Coefficient	28
3.4.5	Error Between Predicted & Actual Data	29
3.5	Damaged Hardware	29

3.6	Lessons Learned	30
-----	---------------------------	----

LIST OF TABLES

1	Team Summary Chart	6
2	Apogee Altitude With Ballast	21
3	Landing Kinetic Energy	22
4	Drift and Descent Time	23
5	Relevant Flight Data	25
6	Masses, Impact Velocities, and Impact Kinetic Energies	27

LIST OF FIGURES

1	The launch site in Brothers, OR.	7
2	FHP Removable Assembly	9
3	Rover wrapped in fiberglass wrap, ready to be attached with Kevlar harness.	10
4	Wrapped rover is attached to retention devices and passed through FHP and fore ballast bay.	11
5	CAD of PEARS integrated into airframe through FHP.	12
6	The final assembly steps on site prior to integrating into the airframe.	12
7	Inserting cellulose wadding as the PEARS is integrated.	13
8	Fore section recovered in brush and snow.	13
9	Landing site too hazardous to deploy rover.	13
10	Payload safely retained throughout entire flight.	14
11	PEARS armed and ready to eject.	15
12	Wrapped rover as it is ejected from the airframe.	15
13	Wrap opening and falling away from the rover.	16
14	Rover fully separated from wrap and bulkheads.	16
15	Rover successfully ejected post-launch and ready to continue its mission.	17
16	Front view of the rover	18
17	Rear view of the rover	18
18	Tangled drogue parachute.	19
19	Zippering damage on aft coupler.	20
20	OpenRocket Ballast Bay Locations	21
21	Descent Trajectory	22
22	Vehicle Demonstration Flight Plot	24
23	Ascent Data	24
24	Descent Data of the Fore Section	26
25	Descent Data of the Aft Section	26
26	Final Drift Locations of Airframe Sections	27
27	The drag coefficient data obtained from altimeters.	28
28	The OSRT re-manufactured the aft coupler to these specifications.	30

ACRONYM DICTIONARY

AGL Above Ground Level. [25](#)

ARRD Advanced Retention and Release Device. [10, 11](#)

ATU Avionics Telemetry Unit. [20, 31](#)

BEAVS Blade Extending Apogee Variance System. [7](#)

CAD Computer-Aided Design. [11](#)

DPST Double Pole Single Throw. [11](#)

FHP Fore Hard Point. [4, 9–12](#)

FRR Flight Readiness Review. [6–8](#)

GPS Global Positioning System. [20, 27, 31](#)

LED Light Emitting Diode. [11](#)

MAC Media Access Control. [20, 31](#)

MPRL Machine Product and Realization Laboratory. [8, 29](#)

OSRT Oregon State Rocketry Team. [4, 7, 10, 20, 21, 25, 29, 30](#)

OSU Oregon State University. [6–8, 29](#)

PEARS Payload Ejection and Retention System. [4, 9–13, 15, 19](#)

PLEC Payload Ejection Controller. [10, 11, 14, 19](#)

RF Radio-Frequency. [19](#)

RRC3 Rocket Recovery Controller 3. [6, 23](#)

RSO Range Safety Officer. [11](#)

SCAR Soil Collection and Retention. [17](#)

SL Student Launch. [7](#)

1 SUMMARY OF FRR ADDENDUM REPORT

1.1 Team Summary

Table 1: Team Summary Chart

Team Name	Oregon State Rocketry Team
Mailing Address	104 Kerr Admin Bldg #1011 Corvallis, OR 97331
Name of Mentor	Joe Bevier
NAR/TRA Number, Certification Level	NAR #87559 Level 3, TRA #12578 Level 3
Contact Information	joebevier@gmail.com, (503) 475-1589

1.2 Purpose of Flight

The flight on March 16th, 2019 served multiple purposes. It primarily served as a Payload Demonstration Flight. In the previous flight on February 22nd, 2019, the vehicle and payload were flown with retention systems active, however payload deployment was not attempted. This flight served as a demonstration of payload deployment and payload mission.

The flight also served as a Vehicle Demonstration Re-Flight to qualify a maximum ballasted launch configuration. The flight on February 22nd, 2019 had 0.0 lbf of ballast in the fore and aft ballast bays. The Vehicle Demonstration Re-Flight featured maximum ballasted condition. The competition flight ballast will be between the minimum and maximum tested ballasted configurations, based on simulations for launch day conditions. Lastly, the Vehicle Demonstration Re-Flight served to qualify a switch in altimeters from StratoLoggerCF PerfectFlite and a MissileWorks [Rocket Recovery Controller 3 \(RRC3\)](#) in each recovery section to dual MissileWorks [RRC3](#) altimeters in each recovery section. The purpose of the altimeter change was based on post flight analysis of the Vehicle Demonstration Flight on February 22nd, 2019, and is detailed in the [Oregon State University \(OSU\) Flight Readiness Review \(FRR\)](#) report.

1.3 Flight Summary Information

1.3.1 Launch Day Conditions

The Payload Demonstration Flight and Vehicle Demonstration Re-flight took place on March 16th, 2019 in Brothers, OR. The launch took place at 2:00 PM, with 0 mph winds as measured by the Pine Mountain Observatory in Bend, OR. Approximately 8 in. of snow was present at the launch site. Shown in Figure 1 is the launch site with snow on the ground. Note the area this image was taken from is the parking and assembly area, which is cleared of all brush. The area the vehicle landed was surrounded by large brush, as shown in Figures 8 - 9.



Figure 1: The launch site in Brothers, OR.

1.3.2 Vehicle Configuration Summary

The flight used a Cesaroni L2375-WT motor, the same motor to be used at competition. Two ballast bays were used to lower the apogee altitude while maintaining stability. The fore ballast bay was 1.746 lbf and the aft ballast bay was 1.834 lbf. The stability margin of the Payload Demonstration Flight was 2.16 calibers.

The active system of the [Blade Extending Apogee Variance System \(BEAVS\)](#) was not armed during the flight. The system was restrained to prevent the blades from deploying during flight. The system will be restrained during the competition flight as it was not successfully tested.

1.3.3 Payload & Mission Summary

The final payload was flown and retained during the flight. The fore section of the launch vehicle landed in brush which is not similar to the conditions which can be expected in Huntsville, AL. Additionally, snow presented a hazard to the payload electronics upon deployment. Therefore, the fore section of the vehicle was carried to an area cleared of brush and the payload deployed on a tarp. Soil collection could not be attempted on a tarp in the snow, so testing at [OSU](#) was supplemented for the soil collection mission completion. Testing of soil collection is detailed in the [OSU FRR](#) report.

1.3.4 Flight Altitude Summary

The [Oregon State Rocketry Team \(OSRT\)](#) is targeting an altitude of 4500 ft. The first Vehicle Demonstration Flight had zero ballast and flew to an apogee altitude of 5,079 ft. OpenRocket simulations were performed to determine the amount of ballast to be used during the Vehicle Demonstration Re-flight. A simulated apogee altitude below 4,500 ft was desired to allow a range of ballast configurations at the [Student Launch \(SL\)](#) competition. With zero mph winds, the apogee altitude of the launch vehicle was simulated to be 4,415 ft with the dual ballast bay configuration. The on-board altimeters measured an apogee altitude of 4,415 ft.

1.3.5 *Off-Nominal Events*

The drogue parachute in the aft end of the vehicle became tangled upon separation at apogee. Therefore, the aft section fell at an unexpectedly high rate of speed until main parachute deployment. The main parachute deployed nominally and allowed the vehicle to land at a safe velocity. However, the high forces during main parachute deployment caused the nylon shock cord to tear into the aft coupler.

1.4 Changes Made Since FRR

The only significant change since [FRR](#) is the re-manufacture of the aft coupler due to damage during flight as described in Section [1.3.5](#). Repair of the part was considered, but it was determined that manufacturing a replacement with the same specifications would better ensure the integrity of the component during competition flight. The replacement coupler was laid up out of fiberglass at the [OSU Machine Product and Realization Laboratory \(MPRL\)](#) in the same replacement has been manufactured with the same material and dimensional specification.

No changes to the design of the vehicle or payload were necessary.

2 PAYLOAD DEMONSTRATION FLIGHT RESULTS

2.1 Payload Retention and Ejection System

2.1.1 System Design

The [Payload Ejection and Retention System \(PEARS\)](#) retains the payload within the fore airframe for the entirety of the flight. It is only released and ejected once given the signal from the ground station. The [PEARS](#) is held within the airframe by the [Fore Hard Point \(FHP\)](#)

2.1.1.1 Fore Hard Point

The [FHP](#) consists of a pass through bulkhead and a radially bolted assembly. The pass through bulkhead is epoxied into the airframe to give a hard point for the [PEARS](#) to press against and create a pressure seal. The radially bolted assembly can be seen in Figure 2. The assembly consists of an aluminum ring and an additively manufactured guiding funnel attached to a plywood bulkhead. The aluminum ring is retained to the airframe with six 10-24 radial bolts, while the bulkhead is retained to the ring with six 1/4-20 bolts. The funnel is retained to the bulkhead with epoxy as well as wood screws. Finally, there are two permanent 3/8-16 bolts through the bulkhead that allow for eye hooks to be placed when inserting or removing the [FHP](#) assembly. The plastic funnel serves to guide the threaded rod of the [PEARS](#) through the wooden bulkhead. The weight of the rover and [PEARS](#) is transferred through the wooden bulkhead, which in turn puts force on the aluminum ring and radial bolts. In atypical flight conditions with an added safety factor, the launch vehicle experiences a maximum of 50 G of acceleration. The [FHP](#) is easily able to retain the [PEARS](#), even in this scenario.



Figure 2: [FHP](#) Removable Assembly

2.1.1.2 Payload Ejection and Retention System

The **PEARS** features three subsystems to meet the requirements: the Payload Wrap Assembly, the **PEARS** Removable Assembly, and the **Payload Ejection Controller (PLEC)**. Once assembled, the **PEARS** integrates into the fore section of the launch vehicle and is retained to the **FHP**.

To aid integration as well as retention and ejection, the rover is wrapped in a fiberglass sheet, capped with bulkheads on either end, and wrapped with a Kevlar harness as shown in Figure 3. The wrap is made of four layers of fiberglass weave. It is flexible enough to easily wrap around and compress the foam tires, but rigid enough to spring flat after ejection. The aft bulkhead is the size of the compressed rover wheel and has small grooves for the Kevlar harness to lay within. The fore bulkhead has the same dimensions as the aft, but with an additional epoxied wood ring in the center that helps to align the wrapped assembly with the **PEARS** removable assembly spacer. The Kevlar harness is $\frac{1}{2}$ in. circular braided tubing. The loops on each end were hand sewn by the **OSRT** using $\frac{1}{32}$ in. Kevlar thread and back-stitching a double box pattern.



Figure 3: Rover wrapped in fiberglass wrap, ready to be attached with Kevlar harness.

The **PEARS** Removable Assembly consists of a $\frac{3}{8}$ -16 aluminum threaded rod that runs throughout the full subsystem. One end has a threaded spacer for the wrapped payload to sit against, and the other end is passed through the **FHP** funnel during integration. The fore ballast bay is secured on the section of threaded rod that sticks through the **FHP**.

Attached to the main bulkhead are the retention devices. For retention redundancy, two L2 Tender Descenders and an **Advanced Retention and Release Device (ARRD)** are used. These devices all contain a small amount of 4F black powder, less than 0.3 g each, which are ignited via an e-match to separate and release the links of the devices when given the signal from the **PLEC**. Should the **PLEC** fail during flight, these retention devices cannot be separated, which actively keeps the payload secured within the airframe for the

whole flight. Two 4F black powder ejection charges are located on the top side of the **PEARS** bulkhead. The primary charge is 1.2 g and the backup charge is 2.0 g. To create a pressure seal in the payload chamber, a Santoprene sheet on the backside of the main bulkhead is compressed against the **FHP** during integration. This pressure seal is needed to eject the wrapped rover assembly from the airframe.

The **PLEC** is armed via a **Double Pole Single Throw (DPST)** switch, accessible from outside of the airframe once the **PEARS** is fully integrated. The switch connects the positive terminal of the **PLEC** to ground through a pull-down resistor in one state. This configuration allows for the e-match igniting capacitor on the **PLEC** to discharge, disarming the system. The switch discharges the controller in 2.72 seconds. The other state of the switch powers the **PLEC**, arming it, and turning on an indicator **Light Emitting Diode (LED)** for verification of armed state. While the **PLEC** is armed, it is waiting to receive a key word which triggers the ignition sequence. Once given clearance from the **Range Safety Officer (RSO)**, this key word can be transmitted from the ground station. To transmit the keyword, the ground station requires an arming switch to be flipped on and the deployment button to be depressed for at least 0.5 s. Once the trigger word is received, the **PLEC** ignites five e-matches sequentially at intervals of 1.0 second, for a total firing sequence of 5.0 seconds. The order of e-match ignition is Tender Descender, Tender Descender, **ARRD**, primary ejection charge (1.2 g) and backup ejection charge (2.0 g).

Once the **PEARS** Removable Assembly and Payload Wrap Assembly have been assembled, they can be connected together via the links on the end of the Kevlar harness to the retention devices. The **PLEC** mount goes through the pass-through bulkhead of the **FHP** and the seal is created between the Santoprene rubber sheet and the pass-through bulkhead face. As the system is integrated, the funnel on the **FHP** guides the threaded rod through the bulkhead. From the fore end of the airframe, the rod is retained to the bulkhead with a washer and 3/8-16 nut. Tightening this nut compresses the Santoprene rubber sheet further, creating the pressure seal. The fore ballast bay is then slid onto the threaded rod and sits against the wooden bulkhead of the **FHP**. It is retained with a 3/8-16 nut. The fully assembled system can be seen outside the airframe, passing through the **FHP** and ballast in Figure 4. For clarity, the **Computer-Aided Design (CAD)** model of the integrated system is shown in Figure 5.



Figure 4: Wrapped rover is attached to retention devices and passed through **FHP** and fore ballast bay.

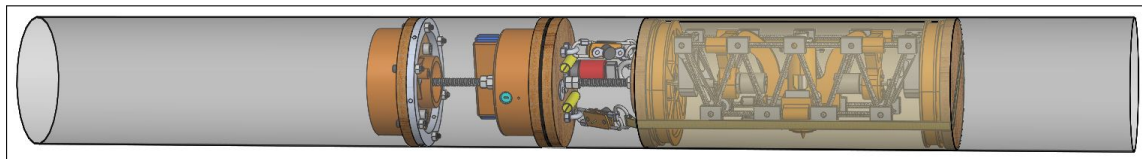


Figure 5: CAD of **PEARS** integrated into airframe through **FHP**.

2.1.2 *Retention and Ejection Performance*

All systems functioned as expected during the launch on March 16th, 2019. No hardware or software failed or required repair. The **PEARS** was assembled and integrated with all components in the final configuration as seen in Figures 6 and 7.



Figure 6: The final assembly steps on site prior to integrating into the airframe.



Figure 7: Inserting cellulose wadding as the PEARS is integrated.

The launch site conditions in Brothers, OR did not allow the team to eject the payload from where the fore airframe recovered. As seen in Figures 8 and 9, the fore section recovered in sagebrush and deep snow. These conditions prevented ejection at the spot of recovery because the snow and brush presented a hazard to the payload and electronics upon deployment. The retention system successfully retained the payload as can be seen in Figure 10. As seen in Figure 8, the aft end of the fore section of the airframe was clear of debris, allowing for the payload to be deployed at the landing site if it were clear of brush and snow as can be expected at the competition launch site.



Figure 8: Fore section recovered in brush and snow. Figure 9: Landing site too hazardous to deploy rover.



Figure 10: Payload safely retained throughout entire flight.

Because the landing site presented a hazard, the **PLEC** was disarmed via the port on the exterior of the airframe, and the fore section of the vehicle was carried to a flat area clear of brush to be deployed on a tarp. The system was then armed again and the ground station was activated, deploying the rover. The deployment process can be seen in the series of images taken from the deployment video in Figures 11 through 15. These figures are still images taken from frame by frame analysis of video capturing the payload deployment. The full sequence from the payload ejection charge being ignited to the payload coming to a stop is less than 2 seconds.



Figure 11: PEARS armed and ready to eject.



Figure 12: Wrapped rover as it is ejected from the airframe.



Figure 13: Wrap opening and falling away from the rover.



Figure 14: Rover fully separated from wrap and bulkheads.



Figure 15: Rover successfully ejected post-launch and ready to continue its mission.

The retention and ejection of the rover was successful as it did not sustain any damage and successfully deployed. The system does not have to be updated further, and ready to be flown in the competition flight.

2.2 Payload Mission

2.2.1 Rover Mission Summary

The rover is contained within the fore section of the airframe. Upon landing, the rover retention devices are released and the rover is ejected from the airframe using black powder charges. It then autonomously travels a distance of 10 ft from the airframe, avoiding objects using sonar modules. Once it is an appropriate distance away, the [Soil Collection and Retention \(SCAR\)](#) system periodically extracts soil from the ground and stores it in the soil retention container until at least 10 mL are stored. After soil retention, the rover autonomously drives to a scientific base station where it performs an additional pH testing experiment.

2.2.2 Rover Performance

Following the mission, the team inspected the rover and determined all components were intact and undamaged. Shown in Figure 16 and 17 are images of the rover following ejection from the airframe. However, the team was unable to perform the soil collection and retention portions of the mission as the launch site contained a foot of snow and and ice. Object avoidance and mobility testing were performed successfully after ejection.

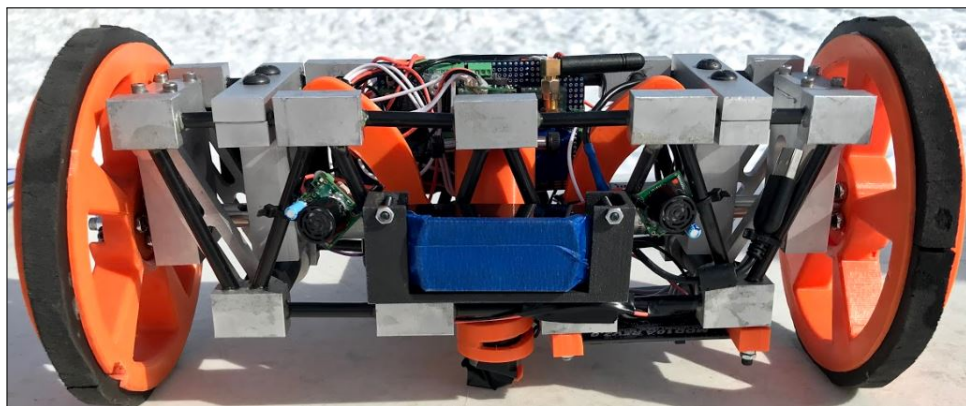


Figure 16: Front view of the rover



Figure 17: Rear view of the rover

2.2.3 Rover Lessons Learned

During mobility testing, the team determined the power supplied to the drivetrain motors should be increased to improve turning capabilities. This can be corrected through software as the motors were not previously set to run at their maximum capability.

3 FLIGHT SUMMARY

3.1 Functional Systems

The launch vehicle performed nearly nominal. During ascent, all systems functioned as intended. During descent, the altimeters functioned properly, separating the vehicle at apogee. At main parachute deployment, the Tender Descenders separated and the deployment bag charges ejected the deployment bag from the airframe. During flight, the payload was fully retained by the [PEARS](#). Upon the fore section being placed in a safe payload deployment area, the payload was successfully deployed via [Radio-Frequency \(RF\)](#) communication from the ground station with the [PLEC](#).

3.2 Malfunctioning Systems

Two systems malfunctioned during the flight for separate reasons. The primary malfunction was a tangled drogue parachute. The tangled drogue parachute is shown in Figure 18. It is apparent that drogue was tangled and unable to inflate during recovery. The tangled drogue parachute was attached to the aft end of the airframe, allowing that section to descend at an uncontrolled rate until main parachute deployment. The descent velocity at main parachute deployment caused unexpected forces on the recovery systems, resulting in the shock cord tearing through a section of the aft coupler. The aft coupler damage was determined to be irreparable. Shown in Figure 19 is the damage to the aft coupler.



Figure 18: Tangled drogue parachute.



Figure 19: Zippering damage on aft coupler.

Additionally, the [Avionics Telemetry Unit \(ATU\)](#)s did not function completely during the flight. The avionics system experienced a significant software issue that resulted in near total failure to transmit and log the [Global Positioning System \(GPS\)](#) the launch vehicle consistently during assembly and flight.

One of the 900MHz transceivers used on the [ATU](#) during regular testing and operation of the system was swapped with a different hardware unit resulting in discrepancies in the [Media Access Control \(MAC\)](#) address configuration of the [ATU](#) software. The latest revision of the code was modified to account for the new [MAC](#) address and tested for 10 minutes of operation which indicated that it was fully functional. On launch day, the system suffered from a buffer overflow error that prevented successful transmission or recording of coordinate data at about 15 minutes of operation after [GPS](#) lock.

On-site modifications were made to the code to clear buffers and free up system resources on the microcontrollers. Attempts at utilizing the last stable revision of the code proved unsuccessful due to the obfuscation of [MAC](#) addresses resulting from the transceiver change. The demonstrated ability of the transceivers to lose and reacquire lock after addressing the the buffer overflow error was incorrectly interpreted by [OSRT](#) as a sign that data logging would occur nominally, while segments of data could be transmitted after the buffer clear. Unfortunately, only short segments of data were logged for the duration of flight due to this error.

A corrective action plan to ensure the malfunctions will not occur again is outlined in Section [3.6](#).

3.3 Mission Performance Predictions

3.3.1 Flight Profile Simulations

OpenRocket was used to determine the predicted apogee altitude with the two ballast bays added to the launch vehicle. The fore ballast bay was 1.746 lbf and the aft ballast bay was 1.834 lbf. Table 2 shows the predicted apogee altitude of the launch vehicle at the Brothers, OR. launch site with wind speeds of 0, 5, 10, 15, and 20 mph winds. At the time of launch on March 16th, 2019 there were 0 mph cross winds recorded by the Pine Mountain Observatory in Bend, OR.

Wind Speed (mph)	Apogee Altitude (ft)
0	4,415
5	4,413
10	4,402
15	4,385
20	4,363

Table 2: Apogee Altitude With Ballast

3.3.2 Stability Margin

The two ballast bay system allows OSRT to maintain a stability margin above 2.0 calibers. The two ballast bay locations can be seen in the OpenRocket simulation picture in Figure 20. The center of gravity location changes by 0.05 in. from the unballasted configuration. The stability margin of the ballast configuration is 2.16 calibers.

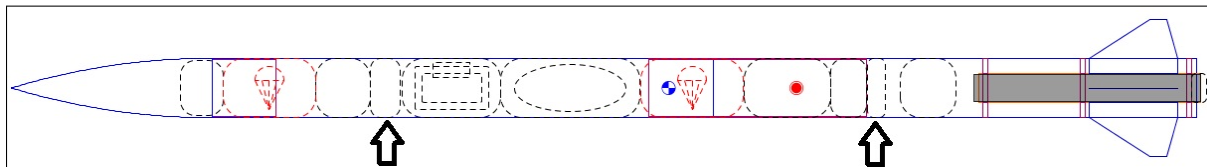


Figure 20: OpenRocket Ballast Bay Locations

3.3.3 Simulated Kinetic Energy

A MATLAB script was used to calculate the landing kinetic energies of each recovered section of the airframe. It was observed through previous launches that the launch vehicle tends to descend slower than the rate simulated, giving the OSRT a small safety factor with these calculations. This is attributed to lowest estimated drag coefficients being used in simulations for the parachutes. The weight, landing velocity, and landing kinetic energy of each section are shown in Table 3. With both sections of the airframe containing

maximum ballast, each sections will hit the ground with a landing kinetic energy less than 75 ft-lbf. The maximum ballast configuration in the fore section of the airframe was limited due to landing kinetic energy.

Table 3: Landing Kinetic Energy

Measurement	Fore Section	Aft Section	Nosecone
Weight [lbf]	18.2	20.1	5.1
Velocity [ft/s]	15.5	14.7	15.5
Kinetic Energy [ft-lbf]	74.9	73.6	19.0

3.3.4 Simulated Descent Time

A MATLAB script was written to calculate the descent time of each section of the airframe. This simulation was verified to be an accurate estimation of descent time by the results of the subscale launches and Vehicle Demonstration Flight. Under a 1.5 ft cruciform drogue parachute and an 8 ft toroidal main parachute for both the fore and the aft sections, the descent trajectories and times for both sections were calculated. This script accounts for the changing air densities at different altitudes, the acceleration of the launch vehicle at apogee and deployment, and the altitude of the launch site in Brothers, OR of approximately 4,600 ft above sea level. The results are shown in Figure 21, with both sections landing in under 90 seconds. The simulated descent times are shown in Table 4.

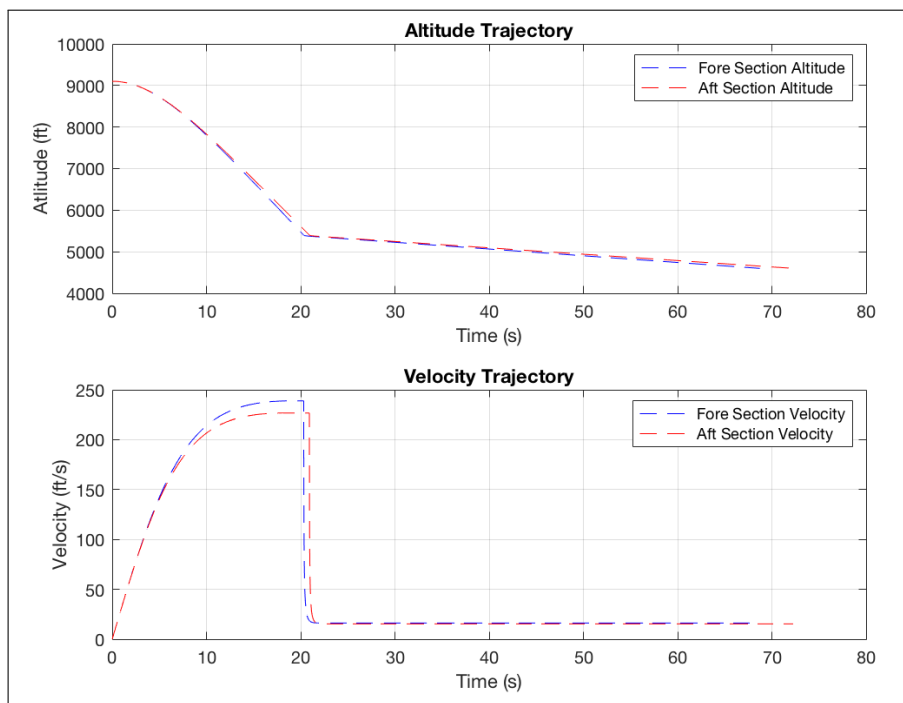


Figure 21: Descent Trajectory

3.3.5 Simulated Drift

A MATLAB script was written to calculate the drift of the descending launch vehicle sections. The wind speed was assumed to be a constant crosswind that does not impact the vertical trajectory. Weather cocking was not included in this calculation, so it was assumed that apogee occurred directly above the launch pad. This is a conservative approach because weather cocking during ascent pushes the launch vehicle the opposite direction of the drift. These calculations are shown in Table 4 along with drift calculations from OpenRocket, which does include weather cocking.

Table 4: Drift and Descent Time

Wind Speed (mph)	0	5	10	15	20	Descent Time (s)
Drift of the Fore Section (ft)	0	478	956	1,434	1,913	65.20
Drift of the Aft Section (ft)	0	502	1,004	1,507	2,009	68.49
OpenRocket Simulation (ft)	2	351	667	1,000	1,441	65.21

3.4 Flight Results

3.4.1 Flight Profile

Four altimeters were flown in this flight, and all four were MissileWorks RRC3 Sport altimeters. All four altimeters functioned properly, logging data throughout the entirety of the flight. Figure 22 shows the flight data logged by all four altimeters. The vertical lines represent when the altimeters fired all ports, igniting ejection charges or separating Tender Descenders. All 12 events are labeled accordingly. Figure 23 shows the altitude, velocity, and acceleration during the ascent of the flight.

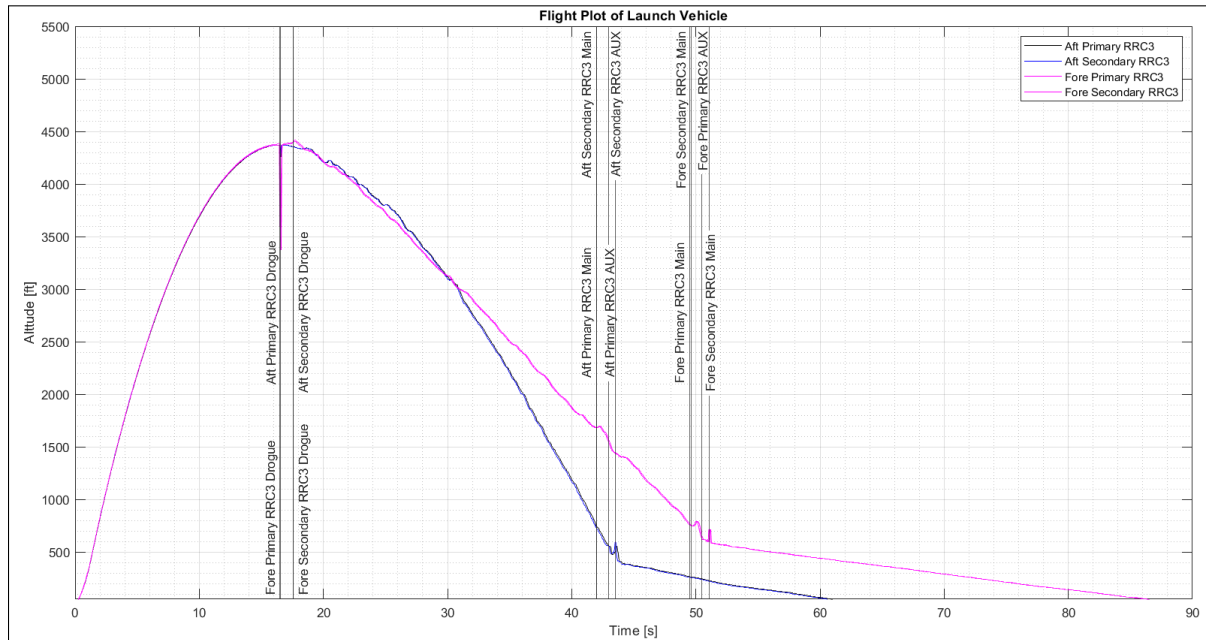


Figure 22: Vehicle Demonstration Flight Plot

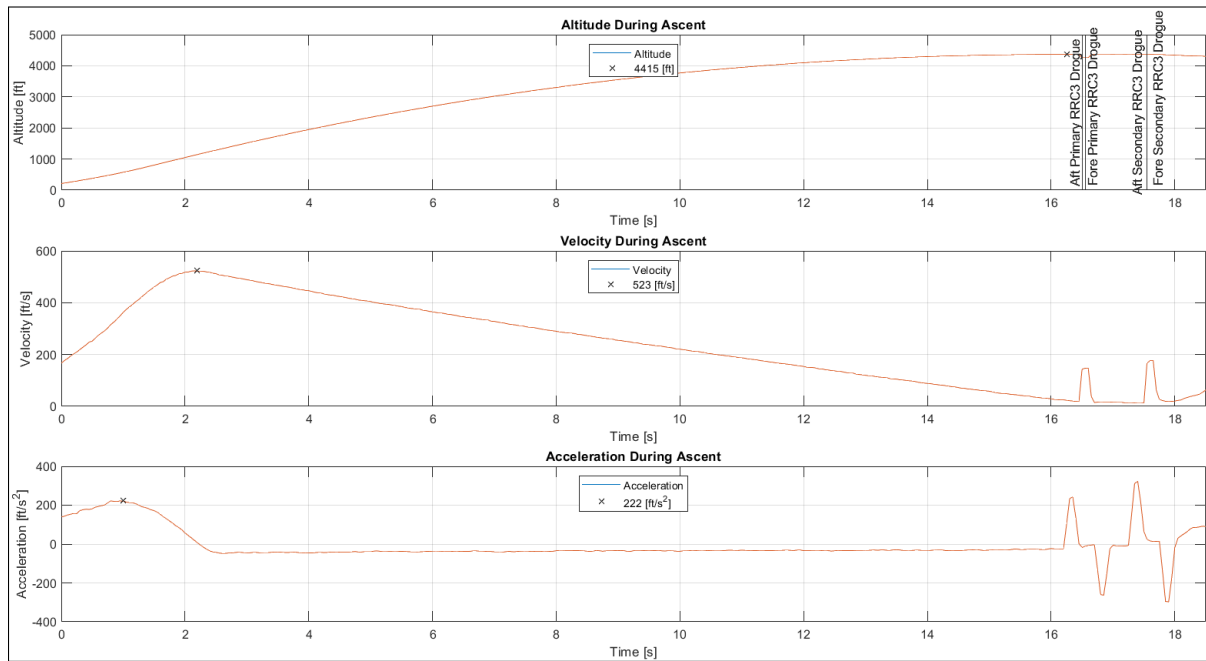


Figure 23: Ascent Data

Table 5 lists the apogee, the time to apogee, and the maximum velocity and acceleration during ascent.

Apogee [ft]	Time to Apogee [s]	Maximum Velocity [ft/s]	Maximum Acceleration [ft/s ²]
4415	16.5	522	222

Table 5: Relevant Flight Data

In the fore section, the primary and secondary separation charges ignited 16.55 and 17.55 seconds into the flight respectively, separating the nosecone from the fore section and releasing the drogue parachute. The Tender Descenders separated 49.55 and 49.65 seconds into the flight at an altitude of 760.7 ft [Above Ground Level \(AGL\)](#). The charges located beneath the deployment bag ignited 1 and 1.5 seconds after the Tender Descenders were released at altitudes of 618.5 and 586.7 ft [AGL](#) respectively. The main parachute inflated around the time the first charge located beneath the deployment bag ignited, leading the [OSRT](#) to believe that it is possible that the main left the airframe without the aid of the deployment bag charges located below it for redundancy.

In the aft section, the primary and secondary separation charges fired 16.55 and 17.55 seconds into the flight respectively, separating the fore section from the aft section and releasing the drogue parachute. This parachute became tangled in the recovery harness. The aft section of the launch vehicle accelerated to the ground reaching speeds over 200 ft/s instead of a controlled descent. The Tender Descenders released at 716.5 ft [AGL](#), 42 seconds into the flight. The charges located below the deployment bag ignited 1 and 1.5 seconds after the Tender Descenders released, 558.7 and 452.5 ft [AGL](#) respectively. The main parachute inflated shortly after the second charge ignited, allowing for a safe descent.

3.4.2 Kinetic Energy and Descent Times

Figures 24 and 25 show the descent data for the fore and aft sections of the launch vehicle. Both the fore and aft sections landed in under the required descent times of 90 seconds. The fore landed in 77.55 seconds, and the aft landed in 50.50 seconds.

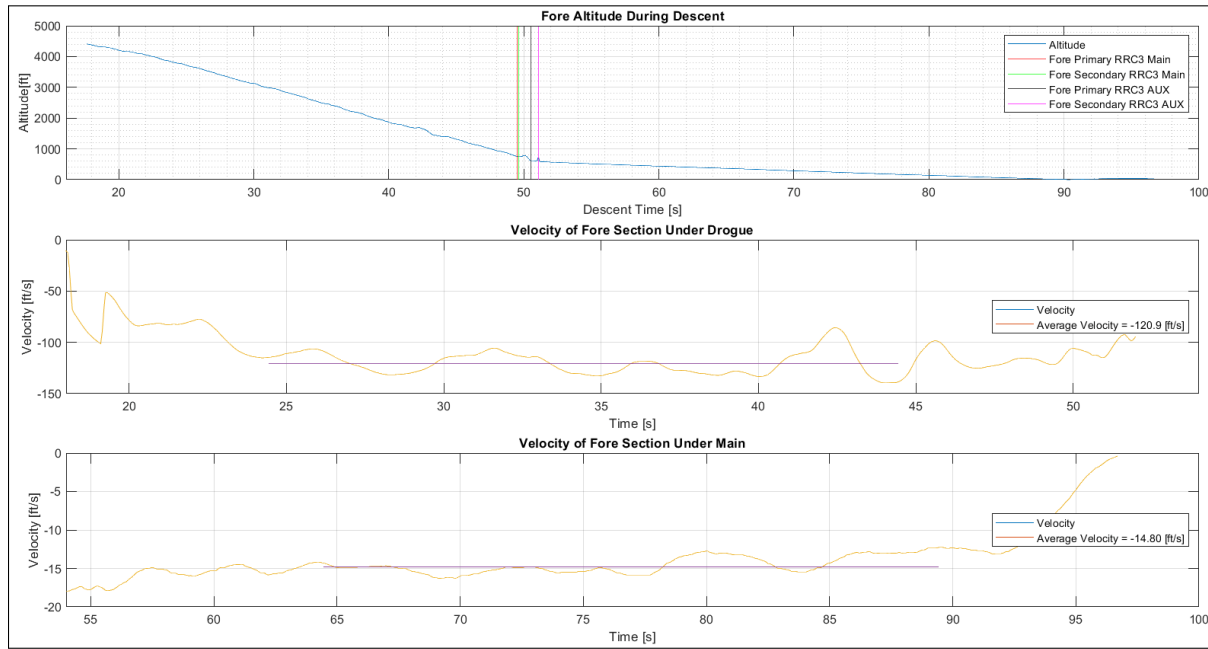


Figure 24: Descent Data of the Fore Section

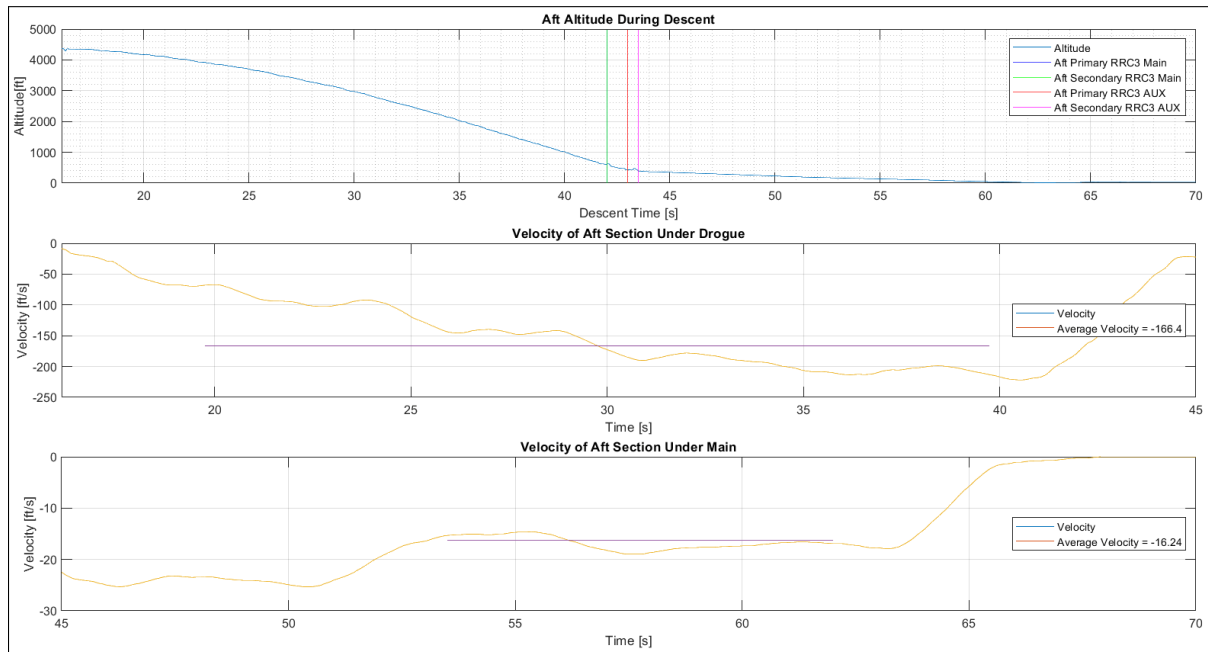


Figure 25: Descent Data of the Aft Section

The average descent rates for the fore section under drogue and main were 120.9 ft/s and 14.8 ft/s respectively. The average descent rates for the aft section under drogue and main were 166.4 ft/s and 16.24 ft/s respectively.

However, due to the aft section never reaching terminal velocity, the average descent rate under drogue is not accurately represented. Table 6 lists the masses, impact velocities, and impact kinetic energies of the aft, fore, and nosecone sections. Impact velocities were calculated by taking the mean of the velocities within two seconds of impacting the ground.

Vehicle Section	Mass [slugs]	Impact Velocity [ft/s]	Impact Kinetic Energy [ft-lbf]
Aft	0.6818	14.30	69.71
Fore	0.6195	13.14	53.48
Nosecone	0.1575	13.14	13.59

Table 6: Masses, Impact Velocities, and Impact Kinetic Energies

3.4.3 Drift

The avionics logged a number of GPS coordinates at their respective landing sites that when corroborated with geographical and topographical data indicate a fore and aft drift radius of roughly 1,400 ft and 1,100 ft respectively. The data collected was not complete enough to render drift plots for reasons described in Section 3.2, but was complete enough to render a map of final airframe section locations.

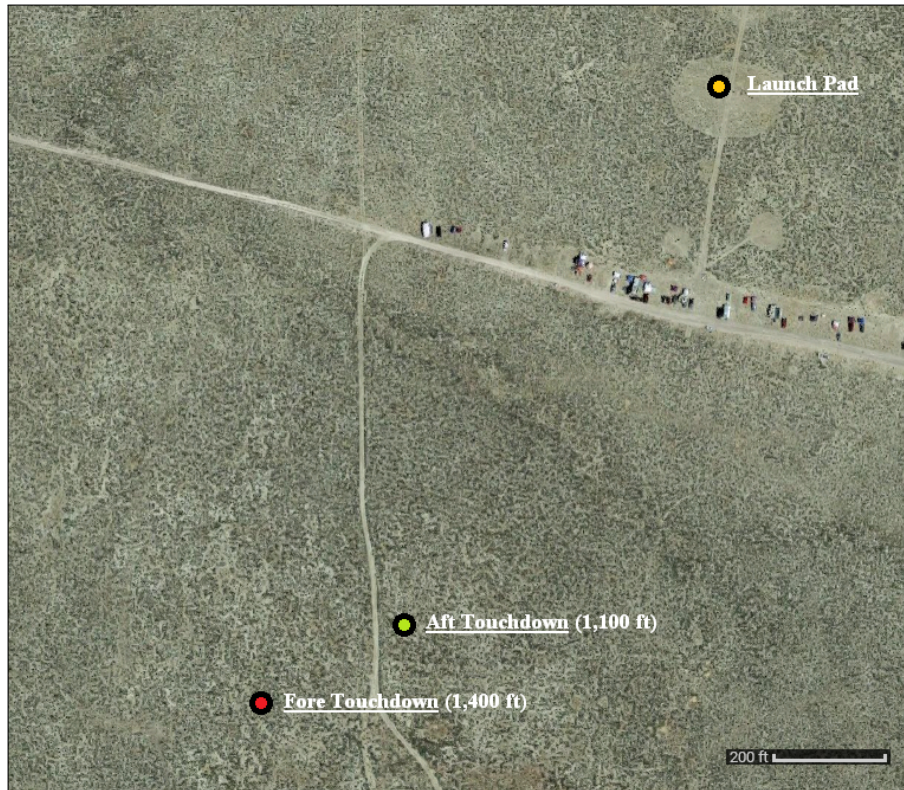


Figure 26: Final Drift Locations of Airframe Sections

3.4.4 Drag Coefficient

The drag coefficient was estimated based on altimeter data to be 0.448 for the flight on March 16th, 2019. Moving average filtering was used to reduce noise in the altimeter data, then data from all four altimeters were averaged to determine an estimated drag coefficient. The reference area was chosen to match the reference area in OpenRocket simulations so the values could be directly compared. The reference area is the cross sectional area of the 6.25 in. diameter airframe, or 30.7 in^2 . A subset of the data was analyzed to determine the drag coefficient. Only data from 5 seconds after takeoff was considered, due to the motor burn. Additionally, data after 10 seconds was not considered due to the flight angle of the launch vehicle becoming significant. As flight angle from a vertical trajectory increases, horizontal velocity increases. The altimeter data only correlates pressure difference with altitude. Therefore, horizontal velocity is not measured or able to be considered in the drag coefficient estimation. In summary, only data from 5 seconds to 10 seconds was considered for all 4 altimeters to determine the drag coefficient. Shown in Figure 27 is the drag coefficient data from the altimeters.

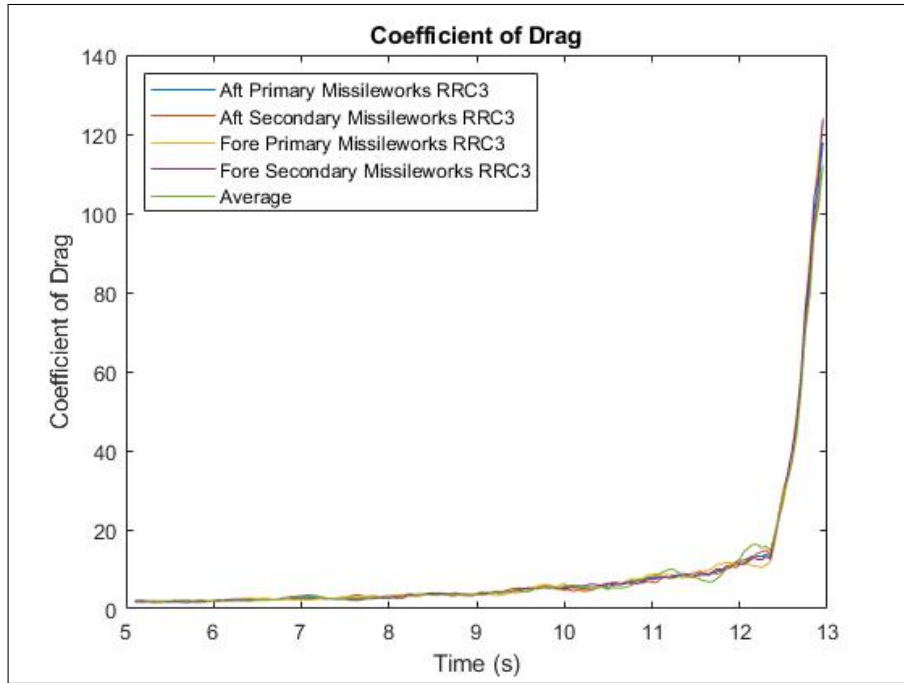


Figure 27: The drag coefficient data obtained from altimeters.

The same process was taken to determine the drag coefficient in the February 22nd, 2019 flight, yielding an estimated drag coefficient of 0.471, a 4.9% difference from the March 16th, 2019 flight. Both values agree well with the simulated drag coefficient in OpenRocket of 0.399, within 15.3% of simulations. The difference

between simulations and actual data can largely be attributed to uncertainty in measurements, especially because only vertical velocity is measured using the altimeter data.

3.4.5 Error Between Predicted & Actual Data

Under the main parachute, both sections fell at a descent rate slower than predicted. This has been the trend for all of the [OSRT](#)'s launches and is attributed to the lowest estimated drag coefficient for parachutes being used in all simulations. The descent time of the aft section of the airframe is much smaller than what was calculated. This is because the drogue parachute was tangled after it was deployed resulting in a faster rate of descent. Both sections drifted significantly farther than predicted, but the drift was still under the maximum drift radius of 2,500 ft. The drift discrepancy is attributed to wind conditions at altitudes above ground level differing from wind conditions at ground level.

3.5 Damaged Hardware

The only hardware damaged as a result of the flight was the aft coupler. This component was determined to be irreparably damaged due to zippering upon main parachute deployment. The component was originally manufactured at the [OSU MPRL](#). A new coupler has been manufactured to the same specifications as the original, ensuring nominal performance during the competition flight. The new coupler was manufactured according to the specifications shown in Figure 28. The materials used for the coupler were 18 layers of fiberglass with an identical layup schedule as originally used.

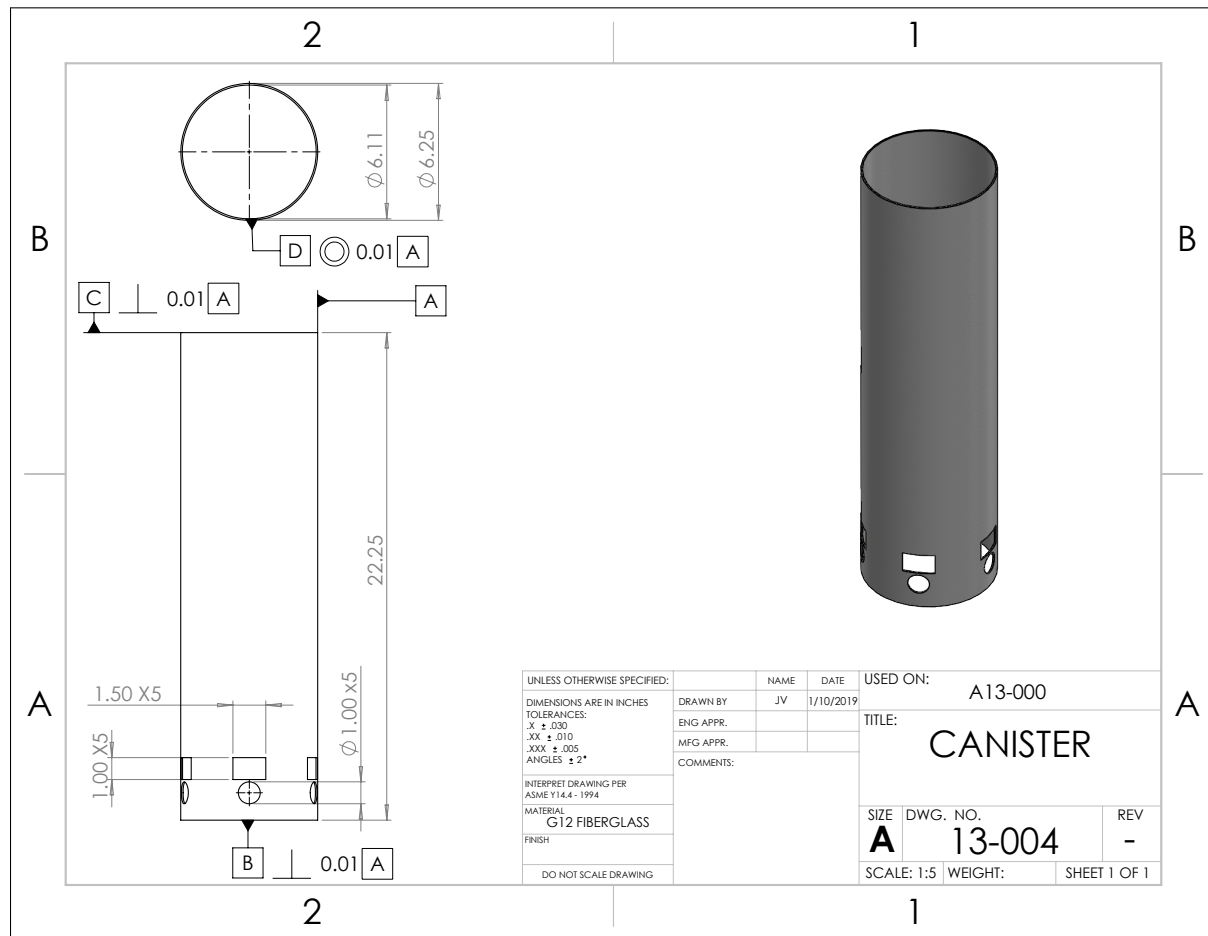


Figure 28: The OSRT re-manufactured the aft coupler to these specifications.

The zippering was a result of the high snatch load when the main parachute deployed. The high snatch load was caused by the drogue parachute becoming tangled upon ejection, resulting in an unusually high rate of descent under the drogue. The fore drogue parachute, however, was packed the same as the aft parachute and deployed successfully. To mitigate this malfunction in future launches additional steps have been added to the recovery integration checklists. The updated procedures will be closely followed and checked by multiple safety personnel.

3.6 Lessons Learned

The primary lesson learned is to pay more attention to detail when placing the risers and drogue parachutes into the launch vehicle. Lack of attention to detail caused a tangled drogue parachute and resulted in the zippering of the aft coupler. It is suspected that the tangled drogue parachute was caused due to packing methods. To ensure this incident is not repeated, additional steps have been added to the packing checklists

which ensure the risers and drogue are neatly integrated into the launch vehicle and placed in the correct positions.

A corrective action plan has been composed to ensure that **ATU** failure to log **GPS** data does not reoccur. The **ATUs** have been reverted to the latest stable release of the code. This code functioned for the duration of full scale assembly, flight, and disassembly of the launch vehicle on February 22nd, 2019. The **MAC** address routing has been modified to account for the 900 MHz transceivers mounted to each **ATU**. These modifications were tested by running and monitoring both **ATUs** for three consecutive hours. The corrective action plan is to complete a test with transmission and data logging for a minimum of three hours prior to all flights. This corrective action plan is incorporated into an updated Prefield Launch Vehicle Checklist.

Any subsequent changes to the **ATU** code base will be tested in the same manner. Once the duration testing has been completed, on-board SD cards are analyzed to ensure that all three hours of consecutive operation have been correctly logged to auxiliary system memory.